Soil Environ. 45(1): xx-xx, 2026
DOI: doi.org/10.25252/SE/2026/254070
Online ISSN: 2075-1141
Print ISSN: 2074-9546

Soil wetting dynamics under subsurface drip irrigation: Influence of soil texture, bulk density, and emitter discharge

Noor Fadhil Salman[1]*, Ezzat Findi Yahya[1] and Zeravan Ariff Abdullah[1]
[1]Department of Soil and Water Sciences, College of Agricultural Engineering Sciences, University of Duhok, Duhok, Iraq
***[Received:** March 12, 2026 **Accepted:** April 30, 2026 **Published Online:** May 04, 2026]*

Abstract

Subsurface drip irrigation (SDI) is an efficient irrigation method widely used in arid and semi-arid regions; however, its effectiveness largely depends on soil physical properties and the resulting soil water distribution. This study investigated soil wetting pattern dynamics under SDI and developed empirical models to predict wetted soil geometry as influenced by emitter discharge, installation depth, irrigation time, soil texture, and bulk density. Laboratory experiments were conducted using two representative soils from the Kurdistan Region of Iraq (Semel—silty clay and Zakho—clay loam). Emitters with discharge rates of 2 and 4 L h^{-1} were installed at depths of 12.5, 25, and 37.5 cm, and equal water volumes (8 L) were applied to monitor the advancement of the wetting front. Nonlinear regression models were developed to estimate maximum horizontal wetted diameter (H) and average vertical wetted depth (V) as functions of emitter discharge (q), irrigation time (t), clay content (c), and bulk density (ρb). The models showed strong predictive performance, with coefficients of determination (R^2) ranging from 0.87 to 0.98. Model validation indicated acceptable accuracy, with root mean square error (RMSE) values of 1.676–5.033 cm, mean absolute error (MAE) of 4.531–10.745 cm, and mean absolute percentage error (MAPE) of 5.468–10.613%. The index of agreement (d) ranged from 0.968 to 0.995, while mean bias error (MBE) values were close to zero, indicating minimal systematic error. The results demonstrated that wetting front expansion was primarily governed by irrigation time, whereas emitter discharge had a comparatively smaller influence, particularly at shallow depths. Increased clay content reduced both horizontal and vertical wetting dimensions, while the effect of bulk density varied with emitter depth. Lower discharge applied over longer durations enhanced lateral water movement, whereas higher discharge promoted vertical flow and deep percolation. The developed models provide practical tools for predicting soil water distribution and can support the optimization of emitter spacing, irrigation scheduling, and water-use efficiency in SDI systems under semi-arid conditions.

Keywords: Wetted soil geometry, Irrigation duration, Clay content, Bulk density

Introduction

Agricultural production in arid and semi-arid regions has very limited availability and quality of water. Improvement of the efficiency of irrigation within the framework of micro-irrigation systems, in particular, drip irrigation, should therefore be considered in terms of sustainable management of water resources (Abdullah, 2022). The subsurface drip irrigation system (SDI) is one of the most significant advancements in drip irrigation technology. This method is characterized by the slow and regular distribution of water to the soil profile via emitters installed along a delivery line beneath the soil surface (Neufeld, *et al*. 1999). Camp (1998) established an empirical approach to forecast the dimensions of the wetted zone of a buried vertical ceramic pipe in a homogeneous porous medium in a variety of soil types under various conditions. It was calculated using initial soil moisture content, drip flow rate, applied head, pipe hydraulic conductivity and irrigation time. The findings showed that the formulas developed were very general and could be applied with a high degree of reliability. Rasheed and Abid (2018) also indicated that the empirical methods were useful in describing the movement of water under buried irrigation systems. Mathematical models can be generally categorized as either analytical, numerical or empirical and empirical equations are useful tools in designing and managing irrigation systems. To obtain optimal wetting geometry, proper emitter discharge and spacing is necessary (Lubana and Narda, 2001). The most important factors that regulate

***Email:** noorfadhil@dpu.edu.krd
Cite This Paper: Salman, N.F., E.F. Yahya and Z.A. Abdullah. 2026. Soil wetting dynamics under subsurface drip irrigation: Influence of soil texture, bulk density, and emitter discharge. *Soil Environ*. 45(1): xx-xx.

water distribution around buried emitters are soil texture, emitter discharge rate, and water uptake by roots (Cote *et al.*, 2003).

One of the most crucial of these factors is the soil texture. Coarse soils tend to promote vertical water movement that can lead to drainage, whereas fine soils tend to promote horizontal soil moisture spreading (Vishwakarma *et al*., 2023). Empirical models tend to be established as functions of applied water volume, emitter discharge and irrigation time as these variables collectively control the redistribution of water around the emitter. Previous studies have shown that the wetted soil volume can be increased with an increase in the discharge rate, but may also result in increased deep percolation losses when irrigation time is not managed (Schwartzman and Zur,

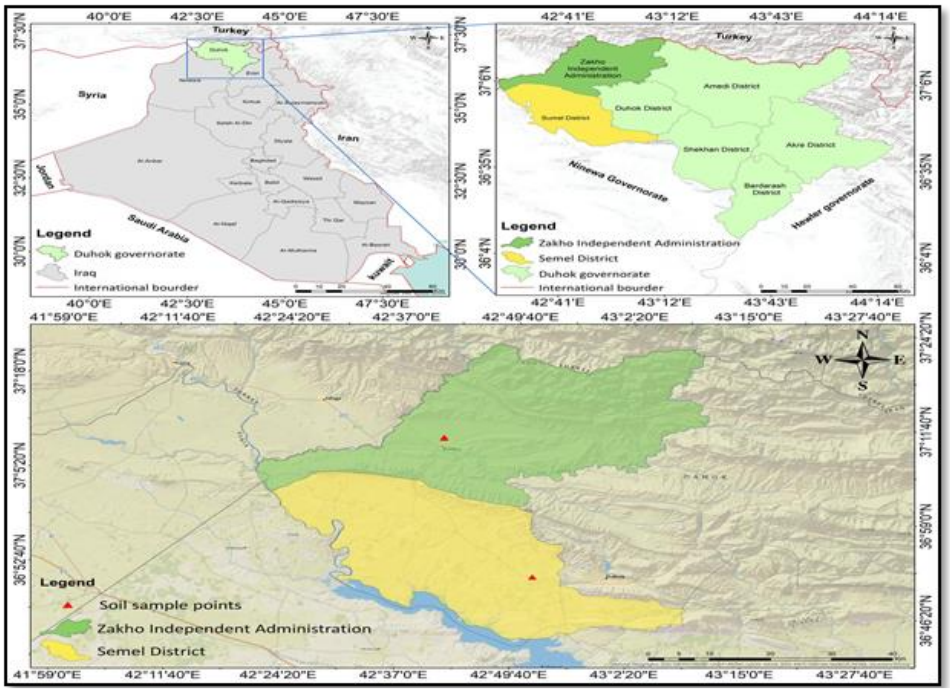

Fig.1. Location map shows the experimental and sampling sites

Table 1. Physical and hydraulic characteristics of the examined soils (Semel and Zakho)

Sample location	Particle size distribution g kg^{-1}			Textural name	Soil Moisture θm%			Bulk density (Mg m^{-3})	porosity (*n*) (%)	Hydraulic conductivity (Ks cm h^{-1})
	Sand	Silt	Clay		-33 kPa	-1500 kPa kPa	θi%			
Zakho	271.5	432.5	296	**Clay Loam**	26.84	16.74	6.06	1.27	52.1	4.22
Semel	43.9	480.1	476	**Silty Clay**	32.13	19.75	6.16	1.38	47.1	3.34

1986). Wetted depth and wetted width are two significant geometrical measures of water distribution that can be used to determine efficient root-zone management and the most suitable time to irrigate (Dasberg and Or, 1999; Ruiz-Sanchez *et al*., 2010). This study has chosen two representative soils of the Kurdistan Region of Iraq, Semel and Zakho due to their agricultural significance. The experimental variables were soil texture, bulk density, emitter discharge rate (2 and 4 L h $^{-1}$), emitter burial depth (12.5, 25 and 37.5 cm), irrigation time and initial soil moisture content. The objective was to quantify the impacts of these interacting factors on wetted width and wetted depth at the same applied water volumes and to establish effective empirical relationships that can be used to enhance the design and management of SDI in semi-arid soils.

Materials and Methods

Soil characteristics

The assessment of soil wetting behavior in this research of subsurface drip irrigation was done on two agricultural soils sampled at the Semel and Zakho Districts in the Kurdistan Region of Iraq; Semel (36°51′27″N, 42°51′42″E), while Zakho (37°9′58″N, 42°41′33″E). Semel site is at an altitude of 467 m above sea level, and Zakho is at 462 m above sea level. Air-dried soil samples were gently crushed and sieved (2 mm) to eliminate coarse particles and large organic debris before packing. The basic physical properties of the soils such as particle size distribution and bulk density were determined using standard laboratory procedures (Table 1).

The dry sieving and pipette methods were used to determine the distribution of the particle size based on the procedure outlined by Gee and Bauder (1986). The core method described by Blake and Hartge (1986) was used in the field to measure soil bulk density. Then, two levels of bulk density were chosen and determined under controlled laboratory conditions in the experimental boxes as outlined in Section (Soil Packing Procedure). Water retention data were obtained in duplicate using pressure plate extractors at (-33, -1500 kPa) (Klute, 1986).

Transparent soil box and hydraulic setup

The wetting behavior in a transparent rectangular box (1.08 m x 1.2 m x 0.10 m) was studied to observe the wetting front of the subsurface emitters in two dimensions. The front was transparent glass, the sides sealed, and the inside walls rough, to avoid flowing preferentially along the edges. To ensure that the operating pressure remained constant in each experimental run, a lateral subsurface drip was fitted to the longitudinal axis of the box and linked to a constant-head water supply (1 bar) through a disc filter, pressure gauge and control valve. (Figure 2).

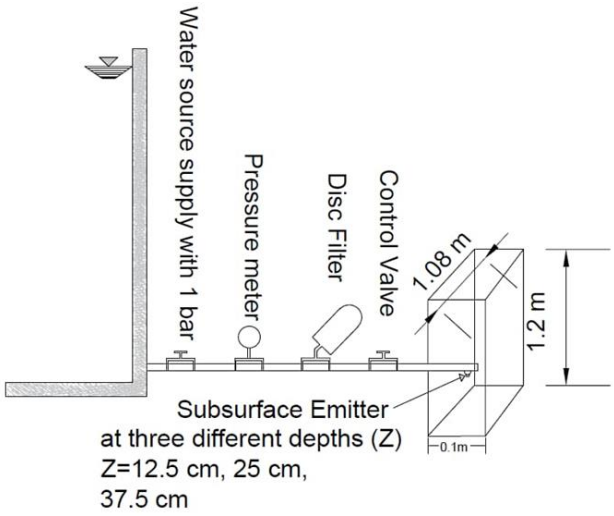

Figure 2: Schematic diagram of the laboratory experimental setup for evaluating soil wetting patterns under subsurface drip irrigation conditions

Figure 3: Illustrations of the laboratory procedure of soil packing that was done to obtain different soil bulk densities

Soil packing procedure

The bulk densities of 1.3 and 1.4 g cm $^{-3}$ were reached by adding pre-weighed soil to the container and compacting it lightly with a wooden tamper to achieve a uniform density of the soil profile. The container was then packed and a 20 cm freeboard was left on top to ensure a flat surface of soil and to create enough space to install the emitter and to move the irrigation pipe. The soil profile was layered four times, 2.5 cm thick. The bulk density of each layer was also

adjusted to ensure that the final bulk density of the soil profile was equal to the target values. The moisture of the soil was kept at the original level during packing to avoid excessive compaction and to preserve the natural soil structure (Figure 3). To avoid disturbance from previous irrigation experiments, the soil was repacked for each combination of soil texture and bulk density.

Irrigation treatments and experimental design

The emitter discharge rates of 2 and 4 L h $^{-1}$ (at an operating pressure of 1 bar) were set at three depths below the soil surface, 12.5, 25 and 37.5 cm, relative to the soil surface to emitter center as illustrated in Figure 1. The experimental design involved two types of soils, two bulk densities, three emitter depths, and two discharge rates, which made 24 experimental units, each with a specific predictive equation. Water was applied at 2 L h^{-1} for 240 min and at 4 L h^{-1} for 120 min, and observations were recorded at 5, 15, 30, 45, 60, 120, 180, and 240 min.

Nonlinear model development

The utilized empirical models allow describing the spatial distribution of applied water both horizontally and vertically, thus providing the ability to describe the geometry of wetting patterns accurately and understand how soil properties, emitter location, and discharge rate affect water flow in the soil profile. The equations are based on the following variables: emitter depth (z, cm), discharge rate (q L h $^{-1}$), clay content (c, %), and bulk density (g cm $^{-3}$). Table 2 shows the model parameters.

Irrigation scheduling and applied water volumes

For the 2 L h^{-1} discharge rate, irrigation water was applied at cumulative times of 5, 15, 30, 45, 60, 120, 180, and 240 min, resulting in a total applied water volume of 8 L. The same total water volume was applied at the 4 L h^{-1} discharge rate; however, the application period was shorter, with observation intervals at 5, 15, 30, 45, and 120 min, permitting direct comparison of wetting behavior under equal applied water volumes and different flow rates. Initially, the discharge rate was tested using a graduated cylinder and a stopwatch, and the collected water volume was measured as a function of time. Subsequently, flow rates were monitored at regular intervals during the irrigation periods, ranging from 5 to 240 min, and the control valve was adjusted accordingly to ensure that the discharge remained within an acceptable range (Figure 4).

Figure 4: Pump–pressure gauge assembly used to provide controlled water pressure for soil box irrigation

Observation and measurement of wetting patterns

The wetting front was monitored using the transparent glass wall of the soil box in every irrigation event. Tracing of the contours of the wetted area was done with a fine permanent marker at the indicated time intervals. Each experimental run included measurement of the maximum horizontal diameter and vertical depth of the wetted bulb relative to the emitter position using a ruler with millimeter resolution. The traced wetting patterns were subsequently digitized to obtain detailed two-dimensional coordinates for further analysis and model calibration. This procedure enabled accurate representation of the wetted soil geometry in both horizontal and vertical directions. Similar experimental approaches for observing wetting patterns in soil containers were reported by Skaggs *et al*. (2004), who compared observed wetting fronts with simulated soil moisture distributions to assess the reliability of experimental measurements. After completing the measurements, the soil in the container was removed and repacked using the same procedure to prepare the next experimental treatment, as illustrated in Figure 5–8.

Results

Development of predictive regression models for the geometry of a wetted front

Empirical regression models were developed to predict the dimensions of wetted soil patterns for the two studied soil textures using multiple regression analysis. The analysis was performed using Microsoft Excel (2021). Several independent variables were included in the regression analysis, namely emitter depth (z), emitter discharge (q), soil bulk density (ρb), and soil clay content (c), which represent the main factors affecting the geometry of the wetted soil pattern. The application of irrigation water was done with a constant operating pressure of 1 bar and a

constant initial soil moisture content. The consistency of initial soil moisture condition reduced the variability of water redistribution, and enhanced the accuracy of the regression models developed.

Figure 5: Six experimental boxes (1-6) labeled for Semel soil, which were designed to test the effects of three emitter installation depths and two different discharge rates for different soil bulk densities. The application period is 240 min

Figure 6: Six experimental boxes (7–12) for Semel soil, designed to assess the effects of three emitter installation depths and two different discharge rates under different soil bulk. densities. 120 min application water

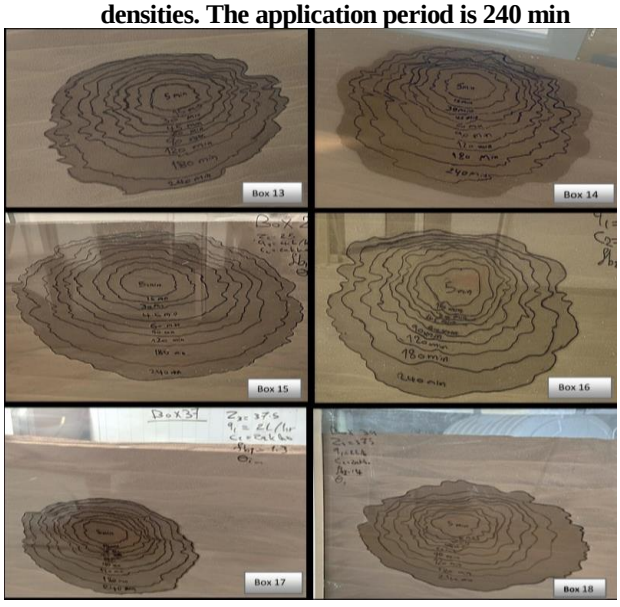

Figure 7: Six experimental boxes (13-18) labeled for Zakho soil, which were designed to test the effects of three emitter installation depths and two different discharge rates for different soil bulk densities. The application period is 240 min

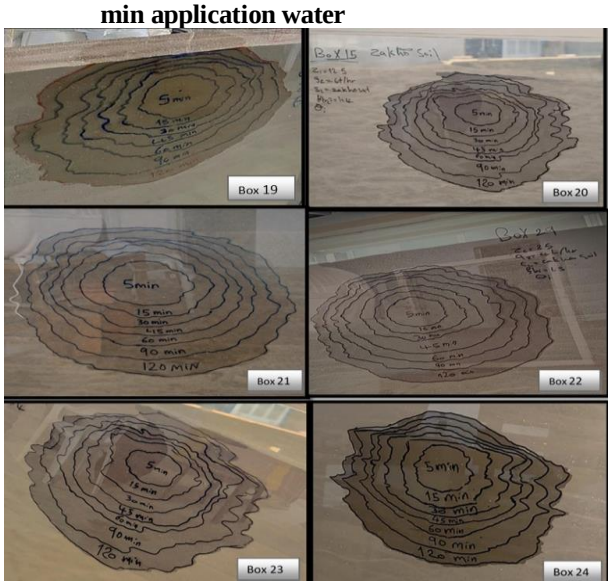

Figure 8: Six experimental boxes (19-24) labeled for Zakho soil, which were designed to test the effects of three emitter installation depths and two different discharge rates for different soil bulk densities. The application period is 120 min

Table 3: Regression coefficient of the developed nonlinear models for predicting maximal wetted diameter and average wetted depth from emitter discharge and depth and some selected soil properties in initial soil moisture content

Response variable	Model code	Type of Model	R^2	RMSE	MBE	MAE	d	CV	CRM	MAPE
Maximum horizontal wetted diameter (cm)	M1	Multiple with nonlinear With four variables	0.87	5.033	-0.137	10.745	0.968	14.54	-0.004	10.613
Average vertical wetted depth (cm)	M2	Multiple with nonlinear With four variables	0.89	3.972	-0.287	10.592	0.972	14.497	-0.010	10.318
Maximum horizontal wetted diameter (cm)	M3	Multiple with nonlinear With four variables	0.97	2.382	-0.051	5.643	0.994	7.081	-0.002	6.566
Average vertical wetted depth (cm)	M4	Multiple with nonlinear With four variables	0.98	1.676	-0.181	4.531	0.995	6.280	-0.007	5.468
Maximum horizontal wetted diameter (cm)	M5	Multiple with nonlinear With four variables	0.96	2.445	-0.215	5.736	0.991	7.524	-0.007	5.849
Average vertical wetted depth (cm)	M6	Multiple with nonlinear With four variables	0.96	2.053	-0.149	5.771	0.991	7.889	-0.006	6.120

Empirical models for wetted pattern dimensions

For an emitter depth (Z=12.5 cm) the wetted pattern dimensions were expressed as:

$$H = 19.63\ q^{-0.028}\ c^{-0.266}\ \rho b^{-0.160}\ t^{0.399}$$
$$V = 21.03\ q^{-0.067}\ c^{-0.376}\ \rho b^{0.009}\ t^{0.418}$$

For an emitter depth (Z=25 cm) the wetted pattern dimensions were expressed as:

$$H = 131.13\ q^{0.089}\ c^{-0.669}\ \rho b^{-2.318}\ t^{0.412}$$
$$V = 78.88\ q^{0.098}\ c^{-0.712}\ \rho b^{-1.067}\ t^{0.423}$$

For an emitter depth (Z=37.5 cm) the wetted pattern dimensions were expressed as:

$$H = 18.09\ q^{0.079}\ c^{-0.419}\ \rho b^{1.762}\ t^{0.372}$$
$$V = 18.32\ q^{0.030}\ c^{-0.448}\ \rho b^{1.296}\ t^{0.386}$$

Statistical assessment of the developed models

Table 3 presents the statistical results for the formulated nonlinear empirical models predicting the maximum horizontal wetted diameter and average vertical wetted depth under different emitter discharges and soil conditions. All models showed high coefficients of determination (R^2) ranging from 0.87 to 0.98, indicating strong explanatory power.

Graphical evaluation of the proposed models

The comparison between observed and predicted values of maximum horizontal wetted diameter and average vertical wetted depth at emitter depths of 12.5, 25, and 37.5 cm is presented in Figure 9–14.

Relationship between irrigation time and wetting dimensions in Semel soil

Figure 15 and 16 show the relationship between irrigation time and wetted dimensions (horizontal radius and vertical depth) in Semel soil (silty clay) under different discharge rates and irrigation periods. Boxes 1 to 6 (Figure 15) were irrigated for 240 min at a low discharge rate of 2 L h^{-1}, whereas Boxes 7 to 12 (Figure 16) were irrigated for 120 min at a higher discharge rate of 4 L h^{-1}.

Relationship between elapsed time and wetting dimensions in zakho soil

Figure 17 and 18 represent the relationship between elapsed irrigation time and wetted radius in Zakho soil (clay loam texture) under different discharge rates and irrigation periods.

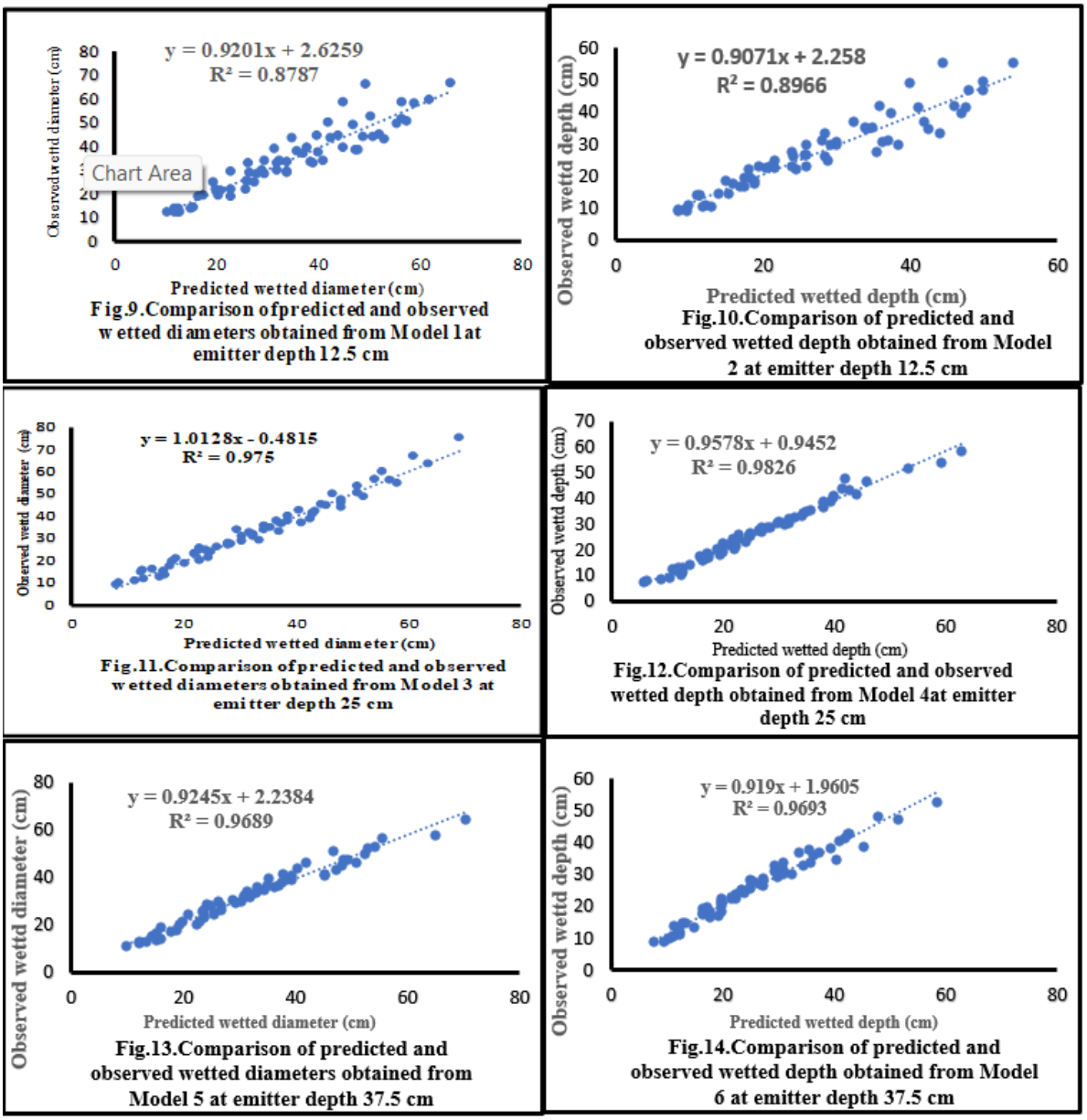

Fig.9.Comparison ofpredicted and observed w etted diameters obtained from Model 1at emitter depth 12.5 cm

Fig.10.Comparison of predicted and observed wetted depth obtained from Model 2 at emitter depth 12.5 cm

Fig.11.Comparison ofpredicted and observed w etted diameters obtained from Model 3 at emitter depth 25 cm

Fig.12.Comparison of predicted and observed wetted depth obtained from Model 4at emitter depth 25 cm

Fig.13.Comparison of predicted and observed wetted diameters obtained from Model 5 at emitter depth 37.5 cm

Fig.14.Comparison of predicted and observed wetted depth obtained from Model 6 at emitter depth 37.5 cm

Spatiotemporal evolution of the wetting front in semel soil (boxes 1–6)

Figure 19 shows how the wetting front of Semel silty clay soil (Boxes 1-6) varies spatially and temporally as irrigation is applied (a total of 8 L applied water volume at 2 L h^{-1}) during 0-240 min. In all cases the wetting front spread vertically and horizontally. At the initial phases (5-30 min), the horizontal expansion close to the soil surface was stronger. The wetting front penetrated deeper and the curvature of the wetting contours was more pronounced after about 60 min. Variation between Boxes 1-6 was interpreted as depth of emitter (z = 12.5, 25 and 37.5 cm) and bulk density (1.3 and 1.4 g cm^{-3}). Increased emitter depths also produced increased wetting patterns and increased depth lateral spread. Increased bulk density had a small effect of increasing the wetted zone. The vertical wetted depth was greater than the horizontal expansion at later irrigation times.

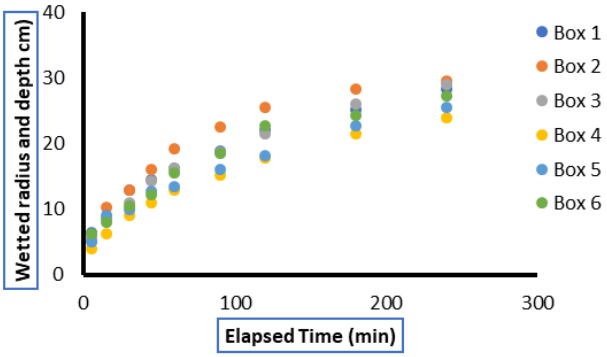

Fig.15 Relationship between elapsed time and wetted radius for Semel soil (silty clay) under different soil boxes (Box 1–6) at a duration of 240 min.

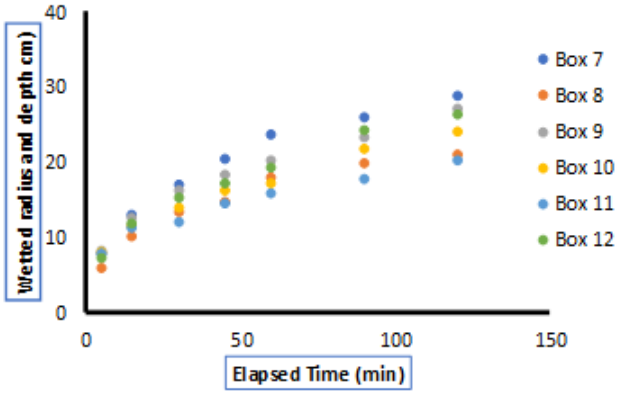

Fig.16 Relationship between elapsed time and wetted radius for Semel soil(silty clay) under different soil boxes (Box 7–12) at a duration of 120 min.

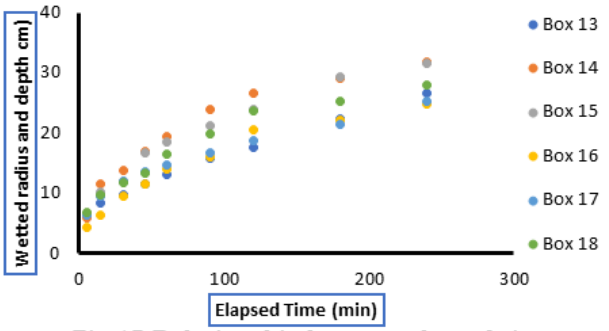

Fig.17 Relationship between elapsed time and wetted radius for Zakho(clay loam) soil under different soil boxes (Box 13–18) at a duration of 240 min.

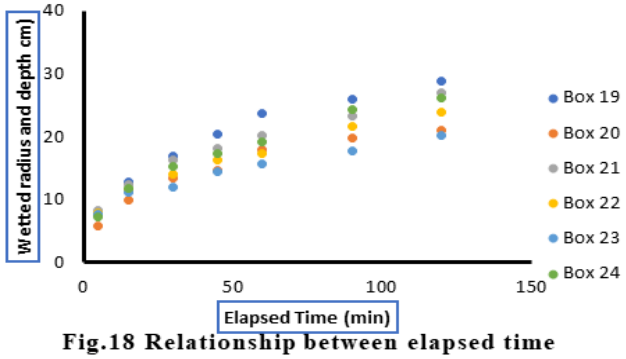

Fig.18 Relationship between elapsed time and wetted radius for Zakho(clay loam) soil under different soil boxes (Box 19–24) at a duration of 120min.

Spatiotemporal evolution of the wetting front in semel soil under high discharge (boxes 7–12)

Figure 20 shows the spatiotemporal changes of the wetting front within Boxes 7-12 of the Semel silty clay soil (0-120 min) of irrigating the soil with a total of 8 L of water at a discharge rate of 4 L h^{-1}. The wetting front progressed down in all boxes, and had a comparatively small lateral expansion. During the first stage (5–15 min), there was minor horizontal expansion on the surface of the soil. The longer the irrigation time was, 30 and 60 min, the further down into the soil profile was the wetting front, and the contours were drawn longer and longer vertically. The difference between Boxes 7-12 was linked to emitter depth (z = 12.5, 25 and 37.5 cm) and bulk density (ρb = 1.3 and 1.4 g cm^{-3}). Boxes with more emitter depths (Boxes 9–12) showed deeper wetting fronts and slightly wider wetted zones at depth. Higher bulk density values were related with a small increase in wetted dimensions. In spite of these differences, there was restricted lateral expansion altogether.

Spatiotemporal evolution of the wetting front in zakho soil under low discharge (boxes 13–18)

The spatiotemporal changes in the wetting front of the Boxes 13-18 Zakho clay loam soil during 0-240 min irrigation are shown in Figure 21 with the sum of applied water being 8 L and the discharge rate being 2 L h^{-1}. During the period of irrigation, the wetting front showed lateral as well as vertical growth in all the boxes. At the first stage (5-30 min), there was pronounced lateral spreading in the area close to the soil surface. The longer the time of irrigation, the deeper the wetting front moved, but its lateral extension continued. Differences among Boxes 13–18 were associated with differences in emitter depth (z = 12.5, 25,

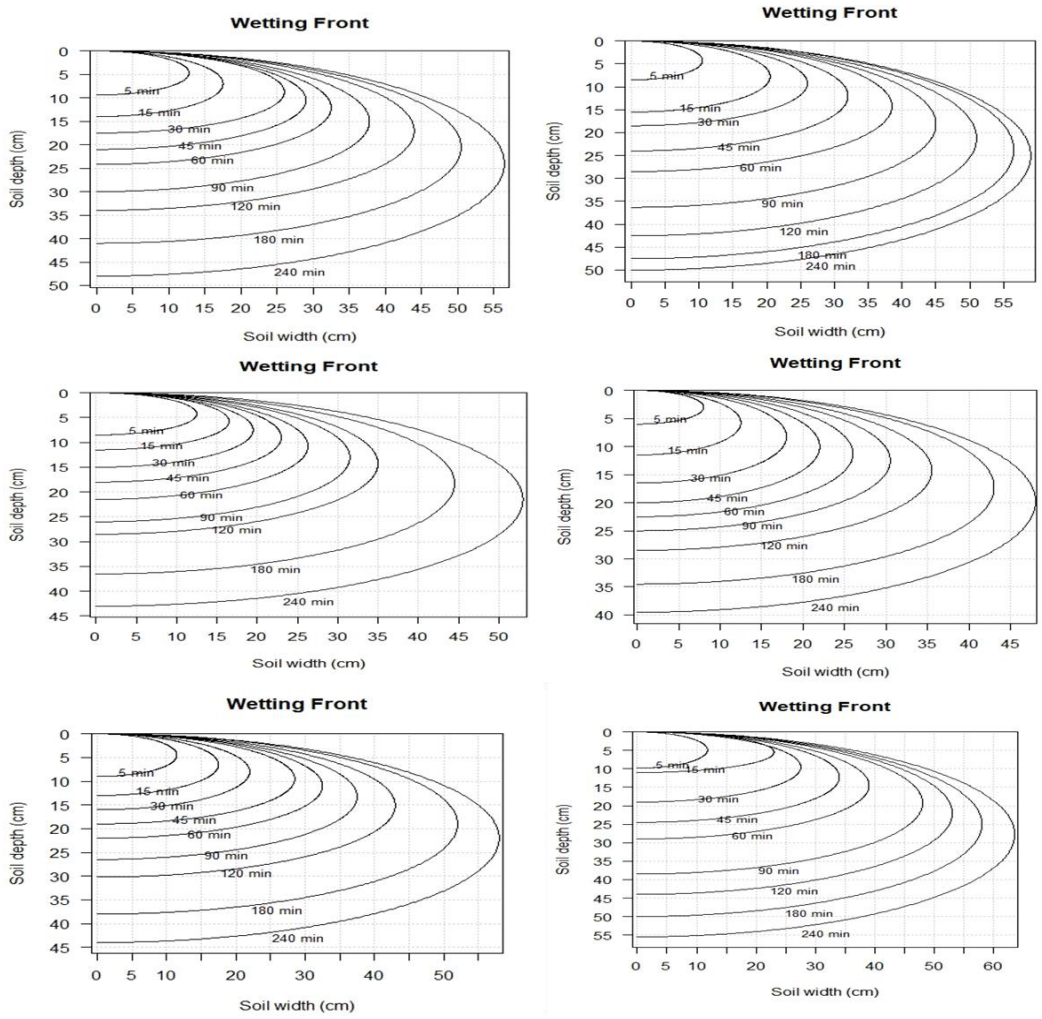

Figure 19: Spatiotemporal distribution of the wetting front in Semel soil for Boxes 1–6 during 0–240 min of irrigation

and 37.5 cm) and bulk density (ρb = 1.3 and 1.4 g cm^{-3}). Boxes with more emitter depths (Boxes 15–18) showed deeper wetting fronts and slightly wider wetted zones at the same observation times. The wetted patterns in clay loam soil had higher lateral expansion under the same discharge conditions as the silty clay soil.

Spatiotemporal evolution of the wetting front in zakho soil under high discharge (Boxes 19–24)

Figure 22 presented the spatiotemporal distribution of the wetting front of Zakho soil (clay loam) at Boxes 19-24 at 0-120 min of irrigation with a total of 8L being applied at a discharge rate of 4 L h $^{-1}$. The patterns of the wetting front in all the boxes were characterized by a fast downward movement with a moderate spreading outward meaning the combination of a high inflow rate and intermediate hydraulic properties of the clay loam soil. With further irrigation after 30 to 60 min, the wetting fronts became more pronounced, and this showed that the influence of gravity was stronger on the movement of the water as the near-surface soil was brought closer to the water level of saturation. Boxes 19-24 differences were primarily due to difference in emitter depth (z = 12.5, 25, and 37.5 cm) and bulk density (1.3 and 1.4 g cm^{-1}). There was a slight increase in wetted areas in boxes with high (ρb). Clay loam exhibited more balanced wetting geometry, in comparison to silty clay of the same discharge conditions, and at later stages, lateral spreading was also observed.

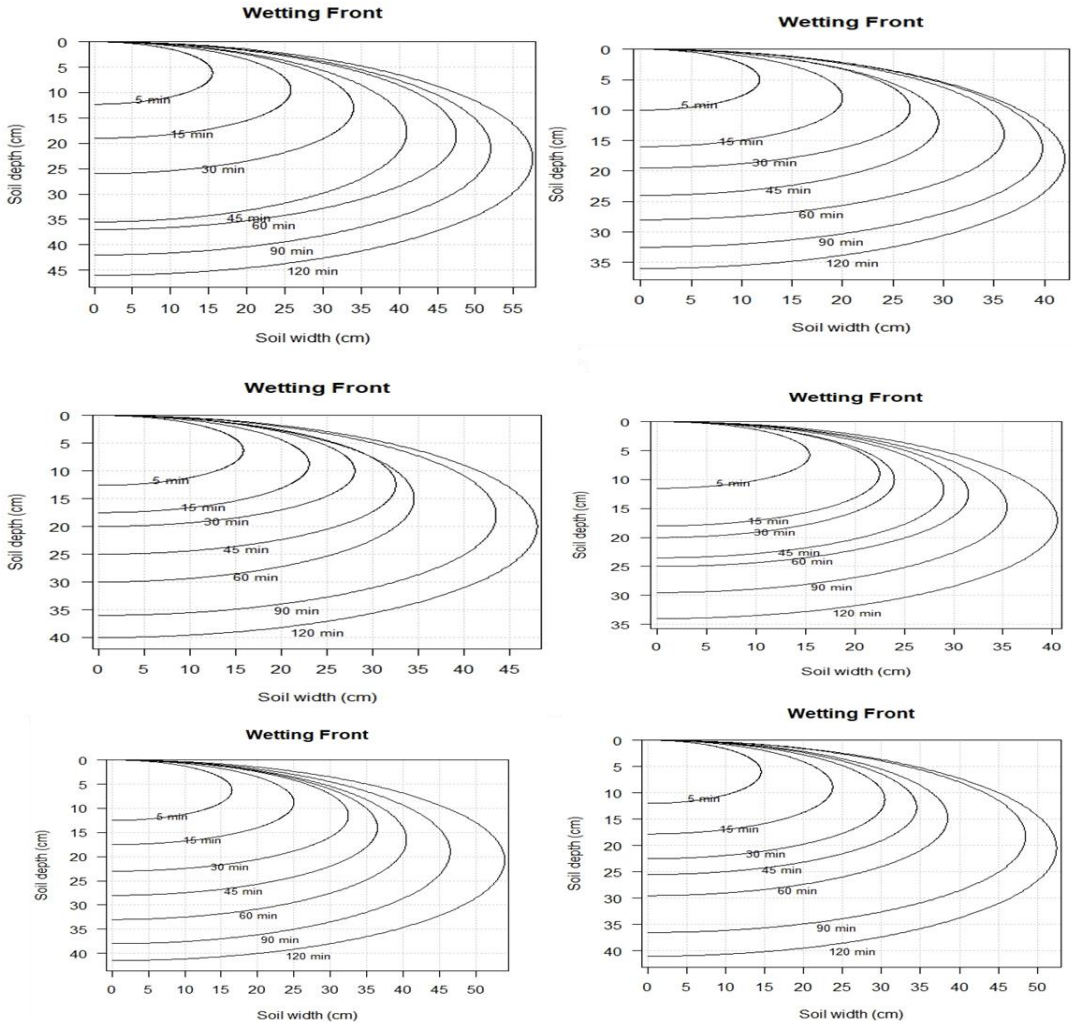

Figure 20: Spatiotemporal distribution of the wetting front in Semel soil for Boxes 7–12during 0–120 min of irrigation

Discussion

In particular, the paper provides research on the dynamics of soil wetting during subsurface drip irrigation, exploring the effects of the soil texture, bulk density, emitter discharge, and installation depth on the wetted soil dimensions. It also seeks to formulate and confirm empirical models to predict the maximum wetted diameter and average wetted depth in semi-arid conditions. The findings are consistent with the unsaturated flow theory, in which cumulative infiltration during redistribution is related to time by a power-law (Philip, 1969). In drip irrigation applied to the surface under the ground, the length of time of application increases the lateral and vertical flow of water under the effects of capillary and gravitational forces, enlarging the wetted soil zone. Both numerical and experimental studies have reported similar trends (Elmaloglou and Diamantopoulos, 2009). Regression analysis was used to develop empirical power-law models to predict horizontal wetted radius (H) and vertical wetted depth (V) of emitter discharges of 2 and 4 L h^{-1} and burial depths of 12.5, 25, and 37.5 cm. The models assign wetted dimensions to discharge (q), irrigation time (t), soil texture parameter (c), bulk density (ρb) and emitter depth (Z) which describes the nonlinear nature of water movement within unsaturated soils (Philip, 1969; Schwartzman and Zur, 1986). Irrigation time (t) always positively impacted H and V at all depths. Exponents of time at 12.5 and 25 cm were

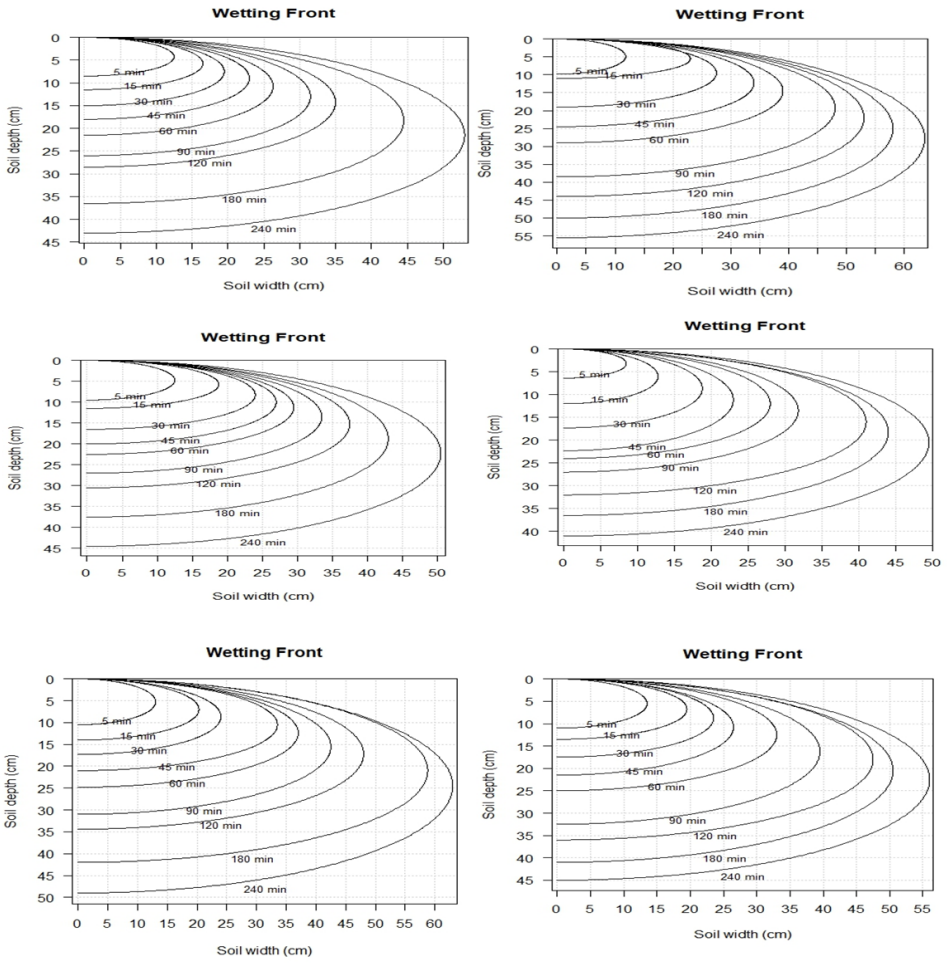

Figure 21: Spatiotemporal distribution of the wetting front in Zakho soil for Boxes 13–18 during 0–240 min of irrigation

0.399 to 0.423 and somewhat less at 37.5 cm (0.372 in H and 0.386 in V) i.e., the wetted expansion was slower at increased depths. The discharge (q) of emitter depended on depth. Discharge exponents were weakly negative at 12.5 cm depth, which means that the wetted dimensions were not very sensitive to discharge. Exponents turned positive at 25 and 37.5 cm, as at 37.5 cm 0.079 (H) and 0.030 (V) were the exponents, with a stronger effect of discharge at deeper placements (Philip, 1969). The soil texture parameter (c) value at all depths (−0.419 to -0.712) was negative, which means that an increase in the clay content decreased the horizontal and the vertical wetted dimension. Bulk density (ρb) had more pronounced impacts at shallow and intermediate depths (12.5 and 25 cm) it had a negative impact on horizontal spread because of decreased porosity, but at 37.5 cm (1.762 in H and 1.296 in V), bulk density had a strong positive impact, increasing wetted dimensions greatly. Such findings indicate a change in depth dominant forces. Capillary forces affect the effect of increased discharge at shallow depths. These results suggest a shift in dominant forces with depth. At shallow depths, capillary forces dominate, limiting the effect of higher discharge. At deeper depths, gravitational forces become more influential, and increased discharge enhances wetted expansion, consistent with previous studies (Keller and Bliesner, 1990; Provenzano, 2007; Cote *et al*., 2003).

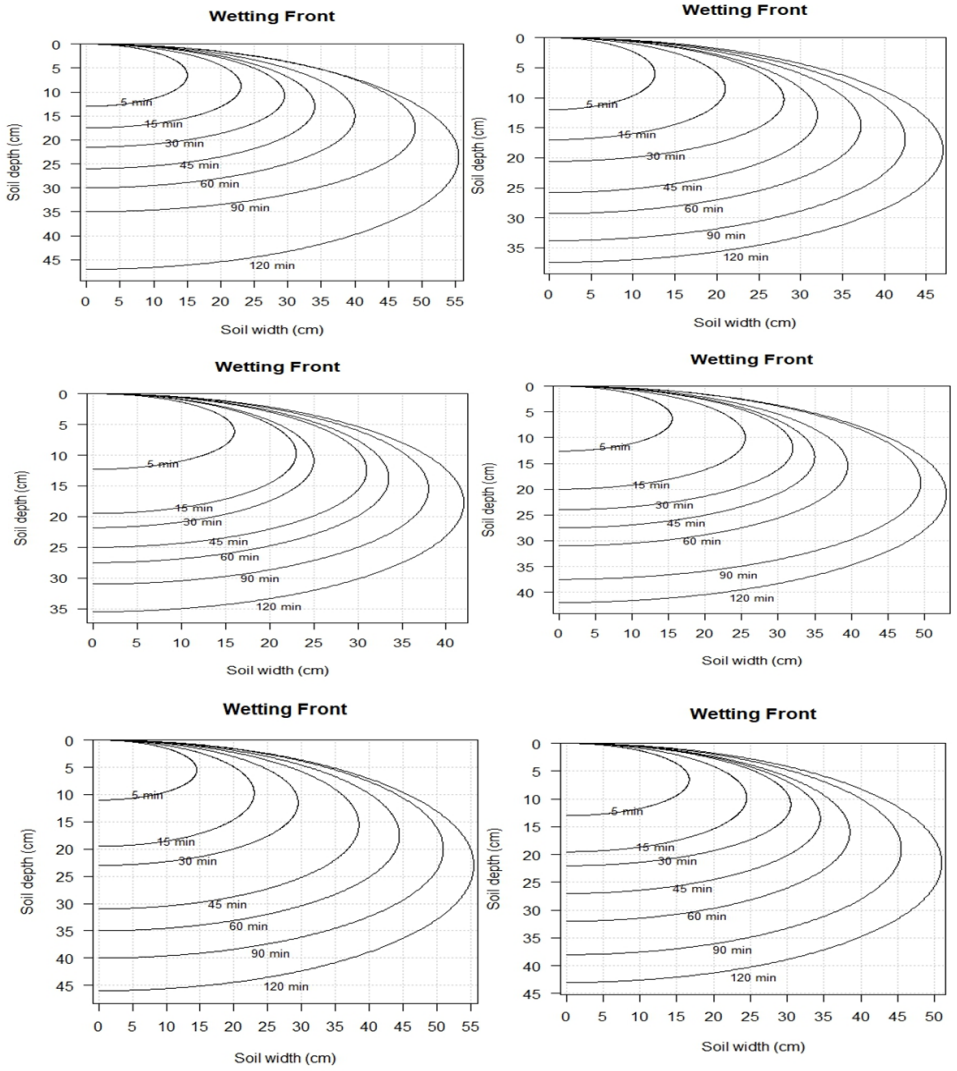

Figure 22: Spatiotemporal distribution of the wetting front in Zakho soil for Boxes 19–24 during 0–120 min of irrigation

The geometry of wetted patterns was consistently affected by soil texture. The negative values of the exponents of the clay content at all depths show that the higher the clay content, the less were the horizontal and vertical wetted dimensions. The saturated hydraulic conductivity of fine-textured soils is also usually lower, the rate of water transmission is slower and the matric effects are stronger than in coarser soils; hence, the wetted bulbs in soils with high clay content tend to expand more slowly and to be relatively small. This observation is in line with earlier researches that found that wetted bulb geometry in drip irrigation is highly influenced by soil texture (Schwartzman and Zur, 1986; Skaggs *et al*., 2004). There was a depth-dependent effect on bulk density. Higher bulk density at shallow and intermediate depths was more likely to inhibit horizontal spread, probably due to the decreased pore continuity and lateral redistribution caused by compaction. Conversely, bulk density at 37.5 cm depth exhibited positive exponents of both horizontal and vertical dimensions indicating that at deeper depths, bulk density was a conditioning variable that affected

redistribution of water. This implies that bulk density must be taken into account when empirically analyzing wetted geometry, especially when the emitters are mounted at a lower location. The comparison between the three emitter depths (12.5, 25, and 37.5 cm) shows that the controlling mechanisms change to the dominant ones. At 12.5 cm depth, capillary forces and irrigation time played the main role in regulating the wetted pattern. At 25 cm depth, discharge rate and soil texture appeared more balanced, resulting in more stable moisture redistribution. At 37.5 cm depth, soil physical properties, especially texture and bulk density, became more influential in determining wetted geometry. This depth-related change supports the concept that shallow placement favors capillary-dominated lateral spread, whereas deeper placement enhances gravity-driven redistribution and increases the influence of soil structural properties (Kandelous *et al*., 2011; Camp, 1998). The statistical of the developed models is also supported by the statistical assessment of the models. The high R^2 and d values along with low values of RMSE and MAE and bias values near to zero indicate that the models were able to give satisfactory prediction of wetted geometry under the conditions tested. This goodness-of-fit has been found to be similar to that of prior drip irrigation wetting experiments and subsurface flow simulations (Schwartzman and Zur, 1986; Skaggs *et al.*, 2004; Kandelous and Šimůnek, 2010). Specifically, the predictive performance of both models M3 and M4 were the best (R^2 = 0.97 and 0.98, respectively), with M1 being the worst, although acceptable (R^2 = 0.87). The values verify that the discharge of emitters and soil physical properties are appropriate predictors of wetting pattern development when using point-source irrigation. This level of goodness-of-fit has been found in earlier research, with the typical range of R^2 being between 0.80 and 0.95 (Schwartzman and Zur, 1986; Skaggs *et al.*, 2004; Kandelous and Šimůnek, 2010). Despite the high values of all R^2, variability between models suggests that there are differences between models in their ability to reflect soil hydraulic behavior. Models M3 and M4 showed higher stability and accuracy compared with M1 and M2, as reflected by lower error values (RMSE = 2.382 and 1.676 cm; MAE = 5.643 and 4.531 cm; CV = 7.081% and 6.280%, respectively). Conversely, the greater values of CV of M1 and M2 (14.540% and 14.497) suggest more variability in prediction in those circumstances. This action is in line with the infiltration theory that indicates that soils that have a homogeneous pore-size distribution, and those with a stronger capillary control, are more likely to generate smoother and predictable wetting fronts (Philip, 1969; Hillel, 1998). Conversely, the soils that are affected by higher gravitational forces and more structural heterogeneity might result in higher variability in water redistribution (Beven and Germann, 1982; Assouline and Or, 2013). The values of RMSE (1.676 cm) and MAE (4.531 cm) show that the predictive accuracy of both vertical and horizontal wetted dimensions is acceptable. The error values were least in model M4, which means that it is very strong in predicting the average vertical wetted depth. The Mean Bias Error (MBE) of most models was between -0.287 and -0.051 with one positive value of 0.149 in M6. These values are near zero, which means that there is low systematic bias. On the same note, Coefficient of Residual Mass (CRM) was between -0.010 and 0.006, which means that the models did not always overestimate or underestimate wetted dimensions. This statistical impartiality is a significant pointer of the dependability of hydrological models (Willmott *et al.,* 1985; Legates and McCabe, 1999). The index of agreement (d) values was also very high (0.968–0.995), indicating strong agreement between measured and predicted values. Model M4 had the greatest agreement (d = 0.995) which validates its predictive power. Also, the Mean Absolute Percentage Error (MAPE) was between 5.468% and 10.613, which means that the prediction errors were acceptable in the engineering field in terms of irrigation design and management. The differences in models imply that there are variations in the quality of the models to describe the hydraulic behavior of soils, however, on the whole, the findings reveal that the equations proposed are statistically sound and hydraulically stable. The models were also validated by the graphical evaluation. Overall, the predictions of vertical wetted depth were almost as accurate as horizontal wetted diameter, again, this physical aspect makes sense since vertical infiltration below a focal source can be more directly controlled by the gravitational gradients and hydraulic conductivity, but the spreading of horizontally occurs more susceptible to the heterogeneity of the soil and the pore that framework (Philip, 1969; Hillel, 1998). In every instance, the data values were close to the regression curves that had been fitted and the result was a high correlation between the measured and predicted values. When the regression slopes are near to unity and comparatively low intercepts, it indicates that there is a narrow systematic deviation and high consistency of the model (Willmott *et al.*, 1985; Legates and McCabe, 1999). The 12.5 cm depth model demonstrated good predictability with R^2 values of 0.878 and 0.896 indicating vertical depth and horizontal diameter respectively. At 25 cm depth, there was greater accuracy with R^2 of 0.975 and 0.983, indicating that the data points well clustered together. At 37.5 cm depth, the models also showed high performance (R^2 = 0.968 and 0.969), indicating that stable predictive performance was maintained even with

deeper emitter placement. At all depths, vertical wetted depth was predicted slightly more accurately than horizontal wetted diameter, as indicated by the higher R^2 values and the narrower spread of points. The temporal development of wetted radius showed a steady increasing pattern with the irrigation time of all the experimental conditions indicating the progressive growth of the wetted soil volume through the accumulated infiltration (Figure 15 and 18). Figure 15 (Boxes1–6; 240 min) showed that the radius was wetted progressively with time, and with higher maximum values than with shorter irrigation times. This means there is increased lateral redistribution with extended water application because longer infiltration period allows the movement of water horizontally after eliminating the vertical infiltration requirements. Figure 16 (Boxes7-12; 120 min) also showed a similar trend except that the maximum wetted radius was relatively less owing to the less time of irrigation, which supports the powerful influence of the application time on the late wetting patterns. In the case of Zakho soil (clay loam), the lateral expansion under longer irrigation period is more pronounced as shown in the Figure 17 (Boxes13-18; 240 min). The variation of Boxes 13-18 can be explained by the diversity of emitter depth (z) and bulk density (ρb) that regulates the hydraulic behavior of soils such as the distribution of pore sizes, their connectivity, and capillary forces. These aspects have direct effect on the ratio between the vertical and lateral movement of water thus impacting on the wetted radius. The same has been observed by Assouline (2002) and Schwartz *et al*. (2010), who stressed the importance of physical properties of soil and the positioning of the emitter in determining the wetting characteristics under drip irrigation. By comparison, with increased discharge rates and reduced irrigation time (Figure 18; Boxes 19-24; 120 min) the wetted radius showed an accelerated early increase and a slow gradual stabilization so that the eventual lateral extent was reduced. This action implies that increased rates of inflow encourage preferential vertical movement because of the forces of gravity and thus limiting subsequent redistribution. As a result, the wetting pattern is even higher vertically even in an identical soil texture. This observation is consistent with the conclusions of previous studies (Skaggs *et al*., 2004; Wang *et al*., 2020), who have stated that higher application rates are likely to decrease horizontal movement and increase the depth of percolation. On the whole, the findings have clearly shown that the duration of irrigation, the rate of discharge, emitter depth and the soil bulk density have a collective control over the wetted radius and wetting geometries. The longer the period of irrigation, the greater is the preference of lateral redistribution and larger wetted radius, and the greater is the discharge rate, the greater the vertical dominance of the flow regime, which restricts the possibility of lateral growth. The findings are consistent with the known infiltration theory and that the optimization of the irrigation design parameters is important to realize the intended wetting patterns and enhance efficiency in water use. The spatiotemporal results confirmed clear differences between soil textures and discharge regimes. When Semel silty clay soil was used with low discharge, lateral redistribution of the wetting front was stronger at the beginning of irrigation because of domination of capillary, and then, the vertical advance was more at later irrigation time as the gravity effect grew. At high discharge, vertical movement was intensified and horizontal growth was relatively weak, which means that the movement towards a gravity-driven flow was accelerated. This is consistent with past research indicating that in fine-textured soils, discharge increases are likely to promote vertical wetting and the potential of deep percolation, but have a small effect on lateral spread (Kandelous and Šimůnek, 2010; Lazarovitch *et al.,* 2006; Šimůnek *et al.,* 2016). Wetting pattern in Zakho clay loam soil was found to be more balanced in terms of vertical and lateral expansion particularly when the discharge was low and the irrigation period was higher. This is representative of the intermediate hydraulic performance of clay loam soil in which the suction of moderation and a comparatively favorable distribution of pore-size enable the lateral redistribution to be more efficient and y*et al*low the gradual downward movement to occur. The wetting front of Zakho soil at high discharge became more oriented vertically but in later stages, lateral spreading was more pronounced compared to silty clay. These findings suggest that the critical controls of wetting geometry and water-use efficiency in clay loam soils are irrigation time and discharge rate (Vishwakarma *et al.,* 2023; Kandelous and Šimůnek, 2010). Practically, the findings reveal that reduced emitter discharge and increased irrigation period tend to enhance lateral redistribution in the active root zone, but elevated discharge enhances the chances of deep percolation, particularly in fine-textured soils. Thus, the nonlinear models developed can be useful in the design of emitter spacing, irrigation scheduling, and water-use efficiency optimization of subsurface drip irrigation. The significance of inclusion of soil hydraulic properties in empirical wetting models is more pronounced especially when trying to extrapolate laboratory observations to the field. Lateral redistribution of water is likely to increase with increased matric suction and capillary forces dominance in fine-textured silty clay soils when applied over an extended period. The disparities between boxes would probably be related to the differences in the burial depth factor (z) and the bulk density (rho), which influence the downward progress and the horizontal expansion of the wetted zone (Schwartzman and Zur, 1986; Shabani *et al.,* 2025).In all

cases, the wetting front moved vertically and horizontally, and this showed how the forces of capillarity and gravity acted together in the movement of water in fine textured soils. During the initial stages (530 min), the lateral redistribution was dominant towards the soil surface, which implies that the capillary forces were dominating because the soils were silty clay with high matric suction. Previous experimental and modeling studies have also reported similar early-time capillary-controlled redistribution with localized irrigation (Lazarovitch *et al.,* 2006; Wang *et al.,* 2020).Once the irrigation time surpassed approximately 60 min, the wetting front was deeper and the curvature of the contour was higher, which means that the flow regime changed to the gravity-dominated flow as surface layers were closer to higher water content and matric gradients were lower. Likewise, greater ρb values slightly expanded the wetted zone, indicating modified pore-scale characteristics that facilitated water infiltration. These findings are aligned with the changes in unsaturated flow modeling in the context of drip irrigation, which indicates the predominance of soil texture in low inflows and extended irrigation times (Šimůnek *et al.,* 2016; Cote *et al.,* 2003).Overall, the findings confirm the hypothesis that with low-discharge irrigation, silty clay soils undergo an initial phase of capillary-dominated lateral redistribution, and a subsequent phase of gravity-dominated deep percolation. This two-phase infiltration characteristic offers a valuable foundation to maximize the emitter spacing and irrigation time in fine-textured soils. The gravitational and matric potential gradient changes are the major factors that affect the transition between these stages. Though the rise in bulk density was linked to a slight advancement of the wetted zone, vertical advancement of the wetting front ultimately surpassed horizontal allocation in the later stages of irrigation, suggesting that the underlying hydraulic characteristics of silty clay was the key factor in determining wetting geometry. The contours of wetting-front advance were found to be strongly downward in all boxes under high-discharge conditions, and with comparatively low lateral dispersion. This can be explained by the fact that the increased application rate shifted the balance between capillary and gravitational forces compared with the situation at low discharge. The wetting fronts at the onset of irrigation still exhibited slight lateral extension at the top of the soil due to the short-term effect of the capillary forces that were related to high matric suction in silty clay soils. But the higher inflow rate soon increased the water content of near-surface soil, decreased matric potential gradients, and led to an earlier change to gravity-dominated flow. The contours deepened and became more vertically stretched, as irrigation was continued to 30 and 60 min, and it was found that redistribution was more and more under the control of gravity, as the upper layers of soil became saturated.

These findings are agree with prior experimental and numerical studies that have found that augmentation of discharge in fine-textured soils primarily augments the rate of vertical wetting, as well as augments the likelihood of deep percolation, but with little benefit in lateral wetted radius (Kandelous and Šimůnek, 2010; Lazarovitch *et al*., 2006; Šimůnek *et al*., 2016).Regarding the irrigation management, these results show that a higher rate of discharge can reduce the time of irrigation but can also cause less lateral wetting of silty clay soils and increase deep percolation losses. This emphasizes the need to maximize the discharge of emitters and irrigation time as a unit and not as individual factors.The behavior observed in Zakho clay loam soil was that of a gradual change of capillarity-dominated flow to a combined capillary and gravitational redistribution as the soil became wet, and matric gradients decreased. Consequently, irrigation time and emitter discharge can be deemed as some of the key controls of wetting geometry and water-use efficiency with the conditions of the study (Vishwakarma *et al*., 2023; Kandelous and Šimůnek, 2010). Boxes with higher depth factors always exhibited deeper wetting fronts and, in certain instances, a little wider wetted region, with increased gravitational effects y*et a*llowing effective lateral redistribution. The reason behind this trend can be explained by the variation in soil hydraulic behavior and redistribution related to the clay loam texture, which are crucial factors in determining the wetted zone under subsurface drip irrigation (Appels and Karimi, 2021; Shabani *et al*., 2025).These results correspond to the recent experimental and numerical data, which show that clay loam soils are favorable to a more balanced lateral and vertical wetting pattern during low-discharge irrigation, which enhances the effective root-zone wetting and minimizes the chances of deep percolation losses (Wang *et al*., 2020). Overall, the wetting patterns indicate that at low discharge, clay loam soils promote slow and relatively even wetting, which is conducive to irrigation practices that are based on longer application times and moderate flow rates to ensure that water is distributed as much as possible in the effective root zone. In the early phase of high discharge (5-15 min) irrigation, the slight yet significant lateral development about the soil surface suggests that the capillary forces initially played a role in the horizontal redistribution even though the discharge was high (Philip, 1969; Hillel, 1998). Nevertheless, the higher rate of inflow soon increased the water content in the upper layers, reduced matric potential gradients and hastened the transition to gravity-dominated flow (Jury and Horton, 2004). The more deeply the emitter is placed, the deeper the wetting fronts and the somewhat more

extended the wetted domains, indicating a greater influence of gravity on downward movement with minimal redistribution at depth (Schwartzman and Zur, 1986).Boxes with higher ρb values exhibited slightly higher wetted areas implying that they had lower resistance to infiltration and the available pore pathways were more accessible to high-flux conditions (Assouline and Or, 2013). Compared with silty clay under similar discharge, clay loam showed a more balanced wetting geometry, and lateral spreading remained noticeable even at later stages because of its lower air-entry pressure and greater unsaturated hydraulic conductivity (Carsel and Parrish, 1988).

Conclusion

In this study, empirical nonlinear models were developed to predict the geometry of the wetted soil zone under the subsurface drip irrigation based on the most important variables of emitter discharge, irrigation time, soil texture, bulk density, and emitter depth. The developed models showed good predictive performance (R^2 = 0.87 to 0.98), low prediction errors (RMSE = 1.676 to 5.033 cm, MAE = 4.531 to 10.745 cm, and MAPE = 5.468 to 10.613%), and good agreement between observed and predicted values (d = 0.968 to 0.995). The results showed that the wetted expansion was largely regulated by the time of irrigation, but the discharge of the emitter had less effect at shallow depths and more at deeper levels. The wetted geometry was significantly influenced by soil texture whereby the greater the clay content, the lower the horizontal and vertical wetted dimensions. Lower discharge rates and longer irrigation periods also preferred water redistribution whereas high discharge rates were linked to short irrigation periods. Overall, the suggested empirical models are practical and valid predictive tools of wetted soil dimensions and can be used to design irrigation systems, optimize emitter spacing, and manage water in subsurface drip irrigation systems, particularly in semi-arid agricultural environments.

References

Abdullah, Z.A. 2022. Evaluation of clogging ratio of drip emitters as affected by different treatments and water quality. PhD dissertation. University of Duhok, College of Agricultural Engineering Sciences, Duhok, Iraq.

Al-Ogaidi, A.A.M., A. Wayayok, M.K. Rowshon and A.F. Abdullah. 2016. Wetting patterns estimation under drip irrigation systems using an enhanced empirical model. *Agricultural Water Management* 176: 203–213.

Appels, W.M. and R. Karimi. 2021. Analysis of soil wetting patterns in subsurface drip irrigation systems – indoor alfalfa experiments. *Agricultural Water Management* 250: 106832.

Assouline, S. 2002. The effects of micro drip and conventional drip irrigation on water distribution and uptake. *Soil Science Society of America Journal* 66: 1630–1636.

Assouline, S. and D. Or. 2013. Conceptual and parametric representation of soil hydraulic properties. *Water Resources Research* 49: 848–867.

Beven, K. and P. Germann. 1982. Macropores and water flow in soils. *Water Resources Research* 18: 1311–1325.

Blake, G.R. and K.H. Hartge. 1986. Bulk density. p. 363–375. In: *Methods of Soil Analysis. Part 1: Physical and Mineralogical Methods*. 2nd Ed. A. Klute (ed.), American Society of Agronomy, Madison, WI. USA.

Camp, C.R. 1998. Subsurface drip irrigation: A review. *Transactions of the ASAE* 41: 1353–1367.

Carsel, R.F. and R.S. Parrish. 1988. Developing joint probability distributions of soil water retention characteristics. *Water Resources Research* 24: 755–769.

Cote, C.M., K.L. Bristow, P.B. Charlesworth, F.J. Cook and P.J. Thorburn. 2003. Analysis of soil wetting and solute transport in subsurface trickle irrigation. *Irrigation Science* 22: 143–156.

Dasberg, S. and D. Or. 1999. Drip irrigation. Springer, Berlin, Heidelberg.

Elmaloglou, S. and E. Diamantopoulos. 2009. Simulation of soil water dynamics under subsurface drip irrigation from line sources. *Agricultural Water Management* 96: 1587–1595.

Gee, G.W. and J.W. Bauder. 1986. Particle size analysis. p. 383–411. In: *Methods of Soil Analysis*. Part 1. 2nd Ed. A. Klute (ed.). American Society of Agronomy, Madison, WI. USA.

Hillel, D. 1998. *Environmental Soil Physics*. Academic Press, San Diego, CA.

Jury, W.A. and R. Horton. 2004. Soil physics. 6th Ed. John Wiley & Sons, Hoboken, NJ.

Kandelous, M.M. and J. Šimůnek. 2010. Numerical simulations of water movement in soil under drip irrigation. *Vadose Zone Journal* 9: 613–625.

Kandelous, M.M., J. Šimůnek, M.T. van Genuchten and K. Malek. 2011. Soil water content distributions between two emitters of a subsurface drip irrigation system. *Soil Science Society of America Journal* 75: 488–497.

Keller, J. and R.D. Bliesner. 1990. *Sprinkler and Trickle Irrigation.* Van Nostrand Reinhold, New York, NY.

Klute, A. (ed.). 1986. *Methods of Soil Analysis.* Part 1. 2nd Ed. Agronomy Monograph No. 9. ASA and SSSA, Madison, WI.

Lazarovitch, N., U. Shani, T.L. Thompson and A.W. Warrick. 2006. Soil hydraulic properties affecting discharge uniformity of gravity-fed subsurface drip irrigation systems. *Journal of Irrigation and Drainage Engineering* 132: 531–536.

Legates, D.R. and G.J. McCabe. 1999. Evaluating the use of goodness-of-fit measures in hydrologic and hydroclimatic model validation. *Water Resources Research* 35: 233–241.

Lubana, P.P.S. and N.K. Narda. 2001. Modelling soil water dynamics under trickle emitters—A review. *Journal of Agricultural Engineering Research* 78: 217–232.

Neufeld, J., J. Davison and T. Stevenson. 1999. Subsurface drip irrigation. Nevada Cooperative Extension, Fact Sheet 97-13. University of Nevada, Reno.

Philip, J.R. 1969. Theory of infiltration. P. 215-296. In: *Advances in Hydroscience*. Vol. 5. V.T. Chow (ed.), Academic Press.

Provenzano, G. 2007. Using HYDRUS-2D simulation model to evaluate wetted soil volume in subsurface drip irrigation systems. *Journal of Irrigation and Drainage Engineering* 133: 342–349.

Rasheed, Z.K. and M.B. Abid. 2018. Numerical modeling of water movement from buried vertical ceramic pipes through soils. *Journal of Engineering* 24: 72–85.

Ruiz-Sánchez, M.C., R. Domingo and J.R. Castel. 2010. Deficit irrigation in fruit trees and vines in Spain. *Spanish Journal of Agricultural Research* 8: S5–S20.

Schwartz, R.C., S.R. Evett and J.J. Casanova. 2010. Soil hydraulic properties and drip irrigation wetting patterns. *Vadose Zone Journal* 9: 969–982.

Schwartzman, M. and B. Zur. 1986. Emitter spacing and geometry of wetted soil volume. *Journal of Irrigation and Drainage Engineering* 112: 242–253.

Shabani, A., A.R. Sepaskhah, M. Golestani and V. Shahabi Zad. 2025. Use of dimensionless time and water volume to estimate subsurface drip irrigation wetted zone in different soil textures. *Scientific Reports* 15: 2397.

Šimůnek, J., M.T. van Genuchten and M. Šejna. 2016. Recent developments and applications of the HYDRUS computer software packages. *Vadose Zone Journal* 15(7).

Skaggs, T.H., T.J. Trout, J. Šimůnek and P.J. Shouse. 2004. Comparison of HYDRUS-2D simulations of drip irrigation with experimental observations. *Journal of Irrigation and Drainage Engineering* 130: 304–310.

Vishwakarma, D.K., R. Kumar, A.S. Tomar and A. Kuriqi. 2023. Eco-hydrological modeling of soil wetting pattern dimensions under drip irrigation systems. Heliyon 9: e18078.

Wang, C., D. Bai, Y. Li, X. Wang, Z. Pei and Z. Dong. 2020. Infiltration characteristics and spatiotemporal distribution of soil moisture in layered soil under vertical tube irrigation. *Water* 12: 2725.

Willmott, C.J., S.G. Ackleson, R.E. Davis, J.J. Feddema, K.M. Klink, D.R. Legates, J. O'Donnell and C.M. Rowe. 1985. Statistics for the evaluation and comparison of models. *Journal of Geophysical Research* 90: 8995–9005.